PHYSICAL REVIEW B VOLUME 16, NUMBER 10 15 NOVEMBER 1977

Optical properties at the absorption edge of $Pt_{0.97}S_2$

C. Mankai and G. Martinez
Laboratoire de Physique des Solides, Associé au Centre National de la Recherche Scientifique, Université Paris VI, 4 Place Jussieu, 75221 Paris Cedex 05, France

O. Gorochov
Laboratoire de Chimie Minérale et Structurale, Associé au Centre National de la Recherche Scientifique, Université Paris V, 4 Avenue de l'Observatoire, 75270 Paris Cedex 06, France

(Received 28 June 1977)

Optical properties of $Pt_{0.97}S_2$ have been studied near the fundamental absorption edge of the semiconductor. Measurements of the index of refraction and of the absorption coefficient are reported for $\vec{E}$ perpendicular and parallel to the $\vec{c}$ axis, and as a function of the temperature. A qualitative band-structure model based on the ligand-field theory is presented. The first electronic transitions are found to be indirect for both polarizations and then are followed by a direct transition mainly allowed for $\vec{E}$ parallel to the $\vec{c}$ axis. The character of these transitions is discussed using the proposed band scheme.

I. INTRODUCTION

$Pt_{0.97}S_2$ crystallizes with the CdI_2 structure (trigonal system $P\bar{3}m1$). The structural units of $Pt_{0.97}S_2$ are composed of platinum atoms in octahedral holes sandwiched between two close-packed planes of sulfur atoms. Whereas the bonding, inside a layer, between platinum and sulfur atoms, is expected to present a mixed covalent-ionic character, adjacent layers are held together mainly by Van der Waals forces, which give a lamellar structure to this compound.

From galvanomagnetic properties[1] this compound exhibits a semiconductor behavior with an activation energy gap of about 0.1 eV.

Zone-center phonon measurements have been reported recently.[2] E_g and A_{1g} modes have been found by Raman experiments at 330 and 302 cm^{-1}, respectively, and infrared-reflectivity measurements give values of 320 and 336 cm^{-1} for E_u (LO), respectively.

Besides this information we do not know much about this compound and practically nothing on the optical properties. However, from an ionic point of view, charge transfer from platinum to sulfur atoms leaves the opportunity to have a gap between the d bands of the platinum. Combining this fact with the layered character of the structure, a very peculiar behavior of the optical properties of the compound is expected.

We shall say few words on the preparation of the samples in Sec. II. Section III will be devoted to the principles of the experiments and Sec. IV to the expected band structure for this material. Results of measurements are presented in Sec. V and they are discussed and interpreted in Sec. VI.

II. PREPARATION OF SAMPLES AND CHARACTERIZATION

Single crystals were prepared by chemical vapor transport in closed quartz tubes 12-mm i.d. and 200 mm long. The charge was an appropriate mixture of Pt(99.99%), S(99.999%) and P(99.999%) in molar ratio 1 : 3 : 1 and 75 Torr of chlorine. The detailed procedure is described elsewhere.[1] Crystals can also be obtained without chlorine but the presence of phosphorus was necessary for the crystal growth.

The crystals were analyzed by x-ray diffraction, density measurements, and electrical resistivity. The CdI_2 structure was confirmed with $a = 3.51$ Å and $c = 5.03$ Å. A composition of Pt_xS_2 was found within the range $0.97 < x < 0.98$ in agreement with previous results from density measurements.[1]

Crystals are always n type with a resistivity of about 1 Ω cm at room temperature, increasing to 10^4–10^5 Ω cm at 40 K. Impurities were analyzed by a mass spectrometric method: small amounts of phosphorus (<25 ppm) were detected. Crystals are obtained as platelets of typically 100-μm thickness and 10-mm^2 surface. They have been peeled to decrease the thickness and to perform optical measurements. The experiments reported here have used five samples with thicknesses 1.6, 2.8, and 32 μm.

We shall omit in the following the subscript x when talking about Pt_xS_2, keeping in mind that all samples are platinum deficient. This fact and the results of impurity analysis lead us to think that samples are highly compensated and that the activation energy ($\simeq 0.1$ eV) found in the resistivity measurements is probably quite different from the intrinsic gap.

If we compare the ratio $c/a = 1.42$ of PtS_2 to the values measured[3] for similar compounds such as PbI_2 (1.53), SnS_2 (1.61), HfS_2 (1.61), and TaS_2 (1.74), it is clear that the value for PtS_2 is much lower than the other ones. Particularly, the sulfur atoms there are far from the arrangement of a perfect hexagonal close packing ($c/a = 1.63$). Another consequence of this low value for c/a is that the distance between the anion planes inside a layer is probably significantly less than twice the ionic radius of S^{2-} (1.84 Å).

III. EXPERIMENTAL PROCEDURE

Due to the wide range of energies investigated at room temperature, we have been led to use different spectrophotometers: a Perkin Elmer 225 spectrophotometer, and a Coderg PHO double spectrophotometer.

A. Measurements of the indices of refraction $n_\perp$ and $n_\parallel$

For layered compounds it is rather easy to use natural or peeled samples to observe interference fringes and then to deduce the index of refraction. In fact, if the ordinary index of refraction ($n_\perp$) is easy to obtain with tolerable precision, the extraordinary one ($n_\parallel$) is much more difficult to measure and requires very careful measurements and precise knowledge of $n_\perp$. For this reason we have used a method recently developed[4] for GaSe that we improved here.

At normal incidence, for an electric field $\vec{E}$ perpendicular or parallel to the $\vec{c}$ axis of the sample, maxima of the interference fringes occur at energies ω (in cm^{-1}) following the classical relation

$$2nd\omega = K , \tag{1}$$

where d is the thickness of the sample (in cm) and K an integer. For some thicknesses of the sample, the first order of interferences ($K = 1$) can be reached in the available range of energies and the variation of the product nd can be followed with a precision of about 10^{-4}. Because this precision is about that which is required to evaluate $n_\parallel$, we are led to find the thickness of the sample with a comparatively equal precision. For oblique incidences at a angle θ, (1) must replaced by

$$2nd\omega(1 - \sin^2\theta/n_i^2)^{1/2} = K , \tag{2}$$

where $n_i = n$ for $\vec{E}$ perpendicular to the $\vec{c}$ axis, and $n_i = n_\parallel$ for $\vec{E}$ lying in the incidence plane.

Whatever the configuration, if we fix the value of ω, K is a function of θ. For $\vec{E} \perp \vec{c}$, Eq. (2) is equivalent to

$$n_\perp^2 d^2 - d^2 \sin^2\theta = K^2/4\omega^2 . \tag{3}$$

Then, if we rotate the sample around an axis perpendicular to the $\vec{c}$ axis and measure $K^2(\theta)/4\omega^2$ as a function of $\sin^2\theta$, we get a straight line with a slope equal to $-d^2$ and a value at the origin equal to n^2d^2. The precision of the measurements is practically determined by that of θ and the number of interferences we observe over a rotation of 90°. This number is a function of the thickness of the sample.

To perform the experiment, the sample is mounted in front of a spectrophotometer on a goniometric head fixed on a synchronous motor. The assembly is adjusted to rotate through an axis perpendicular to the $\vec{c}$ axis and passing through the middle of the sample. The transmission of the sample is recorded at a fixed energy as a function of time (and hence of angle θ). The calibration is delicate but we are helped in comparing spectra obtained for $-\frac{1}{2}\pi < \theta < \frac{1}{2}\pi$ and for $\frac{1}{2}\pi < \theta < \frac{3}{2}\pi$. The angle is then determined with a precision of about 0.2°.

The experiment is reproduced for ten different frequencies, each of them giving a value for d and $n_\perp$. The error for $n_\perp$ is about 10^{-2}. However, we know from (1) the variation of nd as a function of ω and we fit this variation divided by the mean value of d found in the angle-dependent experiment, to the values of $n_\perp$ found directly. So $n_\perp$ is known with an absolute precision which is much better than 10^{-2} and a relative precision of the order of 10^{-4}. We performed the same experiments as a function of θ for $\vec{E}$ parallel to the incidence plane using the relation

$$n_\perp^2 d^2 - (n_\perp^2/n_\parallel^2) d^2 \sin^2\theta = K^2/4\omega^2 . \tag{4}$$

We then get $n_\parallel$ with a precision of 10^{-2}, knowing $n_\perp$ and d. Because of the structure of Eq. (2), we cannot improve very much over this precision and results show a corresponding dispersion.

This kind of measurement can only be done in the transparent region of the sample. In principle, by aluminium-plating the sample and looking at the interferences of reflected light, one could go beyond the absorption edge.[4] However, this can only be done with rather large and thin samples, which we do not have.

B. Measurements of the absorption coefficients $\alpha_\perp$ and $\alpha_\parallel$

Whereas $\alpha_\perp$ is obtained experimentally by standard formulas and techniques, $\alpha_\parallel$ is obtained indirectly from a transmission measurement with an angle $0 < \theta < \frac{1}{2}\pi$ and an electric field $\vec{E}$ in the incidence plane. This experiment gives an effective absorption coefficient α^* for an effective thickness of the sample $d^* = d/(1 - \sin^2\theta/n_\parallel^2)^{1/2}$; $\alpha_\parallel$ is then deduced for each energy from the relation

$$\alpha_\parallel = [(\alpha^* - \alpha_\perp) n_\parallel^2/\sin^2\theta + \alpha_\perp] n_\parallel/n_\perp . \tag{5}$$

The structure of this equation is such that the results for low absolute values of $\alpha_{\parallel}$ are obtained with a poor precision, as we shall see in Sec. V.

Before reporting these results, we shall try to get an idea of what the band structure of PtS_2 should be.

IV. EXPECTED BAND SCHEME OF PtS_2

The band structure of this compound has never been studied. As for other transition-metal dichalcogenides, there are two different approaches to this problem. The one-electron band structure approach has been developed by Mattheiss[5] for $1T$-HfS_2 and $1T$-TaS_2 using the augmented-plane-wave (APW) method. These materials crystallize in the same structure as PtS_2. Another approach of the problem can be done using the molecular-orbital theory or the ligand-field theory. It has been applied to this family of compounds[6,7] with comparatively good results. For a qualitative discussion the latter is more convenient and we shall use it to get an idea of the band scheme of PtS_2.

The electronic configuration of platinum is $[Xe]4f^{14}5d^{9}6s^{1}$ and that of sulfur $[Ne]3s^{2}3p^{4}$. The transfer of four electrons from the platinum to the sulfur atoms fills the p bands of the sulfur, which are expected to be much lower in energy than the remaining filled d levels of the platinum, whereas the metal s-p bands lie well above these levels. In fact, found[5] in these compounds are a strong overlap and covalent-bonding effects between the metal and chalcogen s-p orbitals which result in the formation of chalcogen bonding and antibonding s-p states. The resulting energy separation between the bonding and the antibonding s-p orbitals is generally referred to as the σ-σ^* gap. This gap is of the order of 5–10 eV,[5] and metal d levels lie in this gap.

Each platinum atom is octahedrally bonded to six sulfur atoms. If this octahedron is ideal, the resulting symmetry of the ligand field is O_h and the five d levels are split into a $^2T_{2g}$ level and a ^2E_g level.[7] When the octahedron is no longer ideal, the resulting symmetry is D_{3d} and then the $^2T_{2g}$ level splits into a doubly degenerate ^2E_g level and a $^2A_{1g}$ single level (Fig.1). The relative ordering of these last two levels depends on the relative strength of π and σ bonding between the sulfur p bands and metal d bands. This picture holds for the levels at the Γ point of the Brillouin zone. Going to high-symmetry points at the zone boundary involves an additional splitting due to the crystal field of lower symmetry.

According to the band-structure results for

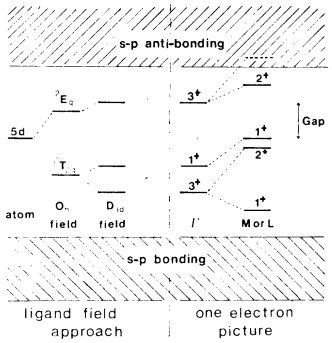

FIG. 1. Proposed band scheme for PtS_2 as deduced from ligand-field theory (left-hand side) and from Mattheiss's work (Ref. 5) (right-hand side).

$1T-TaS_2$,[5] this effect gives to the T_{2g} subband a width of about 3–4 eV, the higher energies being at L or M points (and possibly in the T of S direction). At these points Mattheiss has found the nature of the wave functions of the two upper levels as d_{z^2} and $d_{x^2-y^2}$ and that of the lower level as d_{xy}.

This T_{2g} subband nonoverlaps the upper E_g subband. The actual width of this second subband is more or less blurred by hybridization effects due to the close proximity of the metal $6s$-$6p$ bands. Following Mattheiss, we expect the bottom of the E_g subband at Γ, with wave functions of the d_{xz} and d_{yz} type mixed with $6s$-$6p$ bands at L and M points.

Filling the bands with the available electrons of the compounds, we get a semiconductor with a gap between the T_{2g} and the E_g subbands. This gap is expected to be indirect, the top of the valence band being at L or M points and the bottom of the conduction band at Γ (Fig. 1). Due to the inversion symmetry of the D_{3d} group, the three levels at these points are even under spatial inversion. By parity, the first-order dipole matrix element is expected to be forbidden for direct transitions. The situation is less clear for indirect transitions. This kind of transition can be assisted by odd phonons and then can be slightly allowed.[8] The introduction of spin orbit is not expected to change significantly the qualitative features described above, but could eventually mix the selection rules for the matrix elements with the electric field perpendicular or parallel to the $\vec{c}$ axis for allowed transitions.

V. EXPERIMENTAL RESULTS

A. Index of refraction

Figure 2 presents our experimental results for the ordinary refractive index $n_{\perp}$ at 300 and 85 K. At room temperature, measurements have been

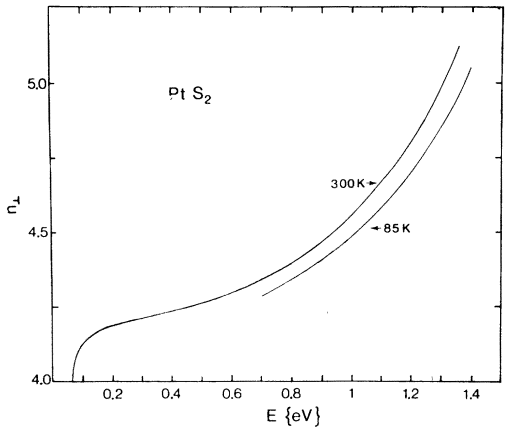

FIG. 2. Ordinary refractive index as a function of energy and temperature.

performed in the far infrared down to the dispersion region of the phonons (0.04 eV). As we can see, between 0.1 and 1 eV, where there is no transition, the dispersion of the refractive index is relatively strong and is due to the influence of the electronic transitions at higher energies. The absolute value of about 4.5 below the absorption edge is also large compared to what is found typically for lamellar compounds: $n \simeq 3$ for GaSe and PbI_2.

The explanation for the high value of $n_\perp$ in PtS_2 probably lies in the fact that the first electronic transitions are lower in energy than those of the other layer compounds. The relative change of $n_\perp$ with temperature at 1 eV is positive: $\partial n/\partial T = 3.5\times10^{-4}$/K, which is very similar to what has been found for GaSe.[9] This value remains constant over a wide range of energies below the optical gap. Characteristic also of the lamellar compounds is the fact that below 85 K, the refractive index does not vary significantly anymore with temperature. This is the reason why the 8-K

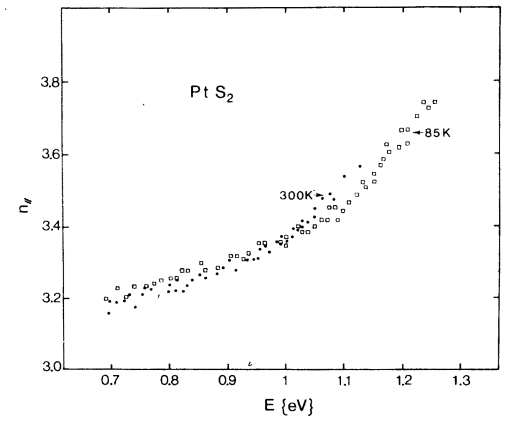

FIG. 3. Extraordinary refractive index as a function of energy and temperature.

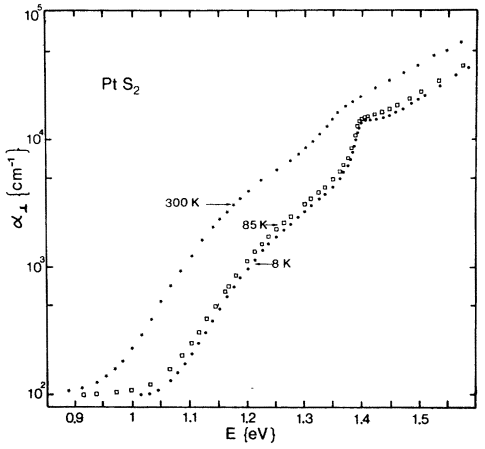

FIG. 4. Variation of the absorption coefficient for $\vec{E} \perp \vec{c}$ as a function of energy and temperature.

curve is not presented in Fig. 2.

On Fig. 3, we give the experimental results for the extraordinary $n_\parallel$ refractive index. As previously indicated in Sec. III, the results are much less precise than those for $n_\perp$. The precision is nevertheless sufficient to get correct values of the absorption coefficient. It is clear also that below the absorption edge the anisotropy of the index of refraction $n_\perp - n_\parallel$ is very large compared to the one found for the other lamellar compounds. We obtain a value around 2 for $\epsilon_{\infty\perp}/\epsilon_{\infty\parallel}$ at 0.8 eV. This result shows that the high-energy spectra of the compound for $\vec{E}$ parallel and perpendicular to the $\vec{c}$ axis should be very different. Another difference between the two polarizations is shown by the temperature dependence of the $n_\parallel$ dispersion curve which is found to be zero below the absorption edge. This seems to prove that the electronic transitions involved in both polarizations are different in origin.

Over an energy range 0.2–0.3 eV above the last measurements of the refractive indices, we used a smooth extrapolation for the dispersion curve of these indices. Different extrapolation schemes have been tried and did not change significantly the calculated variation of the absorption coefficient.

B. Absorption coefficient

Figure 4 gives the results for the $\vec{E}\perp\vec{c}$ absorption coefficient $\alpha_\perp$ at three temperatures: 300, 85, and 8 K. Results for $T = 60$ K have also been obtained, but not one reported on this figure.

The spectra can be divided in three parts. The first one consists in a residual constant absorption coefficient of the order of 100 cm^{-1}. This value depends on the samples and can range from 60 to 140 cm^{-1}. It can be assigned to defects introduced

by departure from stochiometry of the compound or macroscopic defects. Some preliminary photoconductivity measurements, performed down to energies of about 0.3 eV, exhibit a strong response which explains the value of the activation energy gap found in galvanomagnetic measurements. Just for convenience, we set the fixed and mean value of 100 cm^{-1} for $\alpha_\perp$ at low energies for all samples. This procedure does not significantly influence the results at higher energies.

The second part of the spectrum shows a smooth variation of the absorption coefficient as a function of energy over a range of 0.25 eV. The last part is made up of a steplike structure which is not well resolved at room temperature, but is clearly apparent below 85 K.

Similar measurements for different angles of incidence and $\vec{E}$ parallel to the incidence plane have been performed. Using the procedure described in Sec. III, one can calculate the absorption coefficient $\alpha_\parallel$ (for $\vec{E}$ parallel to $\vec{c}$ axis). The results are reported in Fig. 5 for $T = 300$ K and $T = 85$ K. Due to the difficulties of the method, measurements at lower temperatures have not been done. As already pointed out in Sec. III, the uncertainty of these measurements is very large for weak absorption coefficients. They have also been set in such a way that the residual part was of the order of 100 cm^{-1} at low energies. But the way the absorption coefficient increases from this value up to about 1000 cm^{-1} is still too sensitive to all parameters used for calculating it. We give here a mean and "reasonable" set of values obtained on different samples. However different points are well established: For both temperatures the absorption edge for $\alpha_\parallel$ occurs at lower energies than the corresponding one for $\alpha_\perp$. A plateau for a value of $\alpha_\parallel$ around 5,000 cm^{-1} appears clearly. It is then followed by a steplike singularity at an energy which corresponds to that found in the $\alpha_\perp$ spectrum for the same structure. We now try to correlate all the observed features to the expected electronic transitions of the band structure.

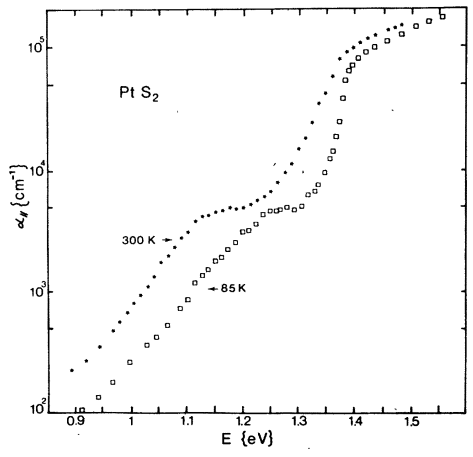

FIG. 5. Variation of the absorption coefficient for $\vec{E} \parallel \vec{c}$ as a function of energy and temperature.

VI. DISCUSSION OF THE RESULTS

A. Results for $\vec{E}$ perpendicular to the $\vec{c}$ axis

Subtracting the residual absorption coefficient from the measured one, we can try to analyze the smooth variation of α versus energy with different analytical laws as this is usually done. To be more accurate, the different theoretical laws are obtained for ϵ_2, the imaginary part of the dielectric constant and not for α. Both quantities are related by $\epsilon_2 = n\alpha/2\pi\omega$, where α and ω are expressed in cm^{-1} units. As we know here the values of n and α, we can get the actual value of ϵ_2. Different power laws of $\epsilon_{2\perp}$ versus energy have been tried and the best fit with straight lines has been obtained in plotting $(\epsilon_{2\perp})^{1/2}$ as a function of the energy. This fit is reproduced on Fig. 6. This can be accepted as a good fit since it spans an energy range of about 0.2 eV and almost two orders of magnitude for α. It corresponds to the analytical relation

$$\epsilon_{2\perp} = A(n(\hbar\omega_q) + 1)(E - E_{g\perp} - \hbar\omega_q)^2 , \qquad (6)$$

typical of indirect transitions with emission of a

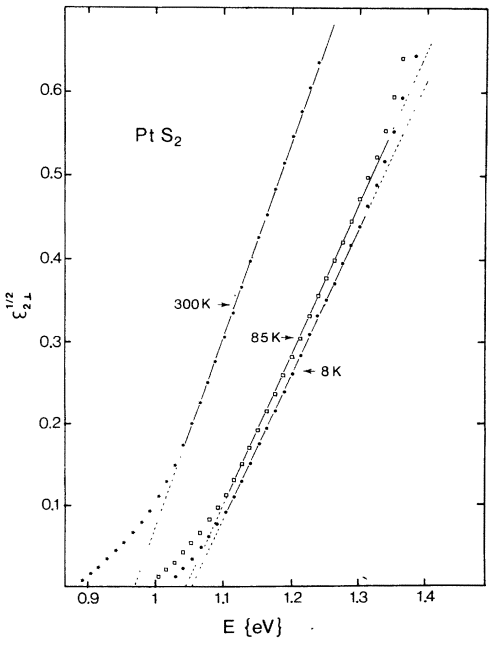

FIG. 6. Decomposition of the imaginary part of the dielectric constant for $\vec{E} \perp \vec{c}$ as a function of energy and temperature.

phonon with energy $\hbar\omega_q$. The corresponding relation with the absorption of phonons gives rise to a tail, on the low-energy side, which should vanish at low temperatures. We do not observe such a behavior and that could be interpreted as the occurance of tail states due to impurities and nonstochiometry in the compound. Due to this effect, the standard procedure to deduce the value of the gap cannot be applied. However, if we assume that the density of states and the matrix elements do not change significantly as a function of the temperature, we can compare the slopes of the $(\epsilon_{2\perp})^{1/2}$ curves versus energy at 300 and 7 K. The square of the ratio of these slopes is equal from (6) to $n(\hbar\omega_q, 300\text{ K})+1$ since $n(\hbar\omega_q, 8\text{ K})\simeq 0$. We can get the value of the phonon energy in this way and we found $\hbar\omega_q = 185 \pm 5\text{ cm}^{-1}$. This value is much lower than all $q \simeq 0$ phonon values which range between 300 and 340 cm^{-1}. Since Eq. (6) corresponds to an indirect process of absorption, the phonon involved in this process would correspond to a zone-boundary phonon. The way expression (6) is obtained theoretically[10] shows that it is characteristic of an indirect transition with allowed components for the matrix elements in three dimensions or forbidden components in two dimensions. From the discussion in Sec. IV about the expected band scheme around the fundamental absorption edge, we keep the idea that the first transition should be indirect between the Γ or L point of the valence band and the Γ point of the conduction band.

To see this transition, and due to the even parity of both conduction and valence states (see Fig. 1), it is necessary to assume the transition assisted by an odd parity phonon. Assuming the top of valence band is located at M, this phonon should belong to the odd irreducible representations M_1^- or M_2^- at the M point of the Brillouin zone. The selection rules for indirect transitions[11] applied here, show that both M_1^- and M_2^- phonons can assist the transition.

We have performed the symmetry analysis of the dynamical matrix at the M point of the Brillouin zone and found that this class of crystals has two M_1^- and four M_2^- phonons for which displacement of atoms are well separated. One M_1^- phonon and two M_2^- phonons involve only displacement of platinum, the other ones only that of sulfur atoms. Due to the large difference between the masses of the atoms, it is expected that the phonons involving a displacement of platinum are the acoustical phonons, and are the phonons which can assist the transition since the initial and final electronic states are platinum d states. Besides this qualitative information we also know that the energy of the phonon involved in the perpendicular polarization is lower than the one involved in the parallel polarization (see Sec. VI B) so the phonon should be a TA phonon (M_1^- or M_2^-). All this discussion provides a necessary condition to make the transition possible. Its actual strength can only be determined by a band-structure calculation which could also answer the question of the two-or three-dimensional character of the transition.

The indirect gap $E_{g\perp}$ is found to be 1.03 eV at 8 K; its temperature variation will be discussed later in Sec. VI C.

At higher energies, a steplike structure appears. The way the absorption coefficient varies with energy excludes *a priori* a forbidden transition for this structure. So we can assume that at least one of the levels involved here is quite different in nature from those appearing at lower energies. Because the valence bands are expected to be d like around platinum over a wide range of energies, we are led to think that this new critical point involves some p level in the conduction band. Using this fact, it is reasonable to think that the conduction levels involved in the forbidden transition and the allowed one, are topologically disconnected and that the contributions of the two transitions to the total dielectric constant $\epsilon_{2\perp}$ are independent. Because they are also additive, we can get the $\epsilon'_{2\perp}$ contribution of the steplike structure. This is done by substracting from the experimental value of $\epsilon_{2\perp}$ the extrapolated contribution of the indirect gap calculated from the linear fit up to 1.45 eV.

The results are plotted in Fig. 7. The structure is clearly resolved below 85 K, but not very well at room temperature where the indirect-gap contribution is very important. This structure appears

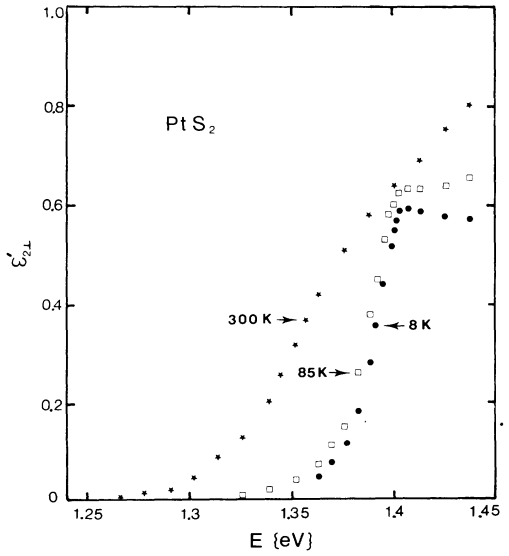

FIG. 7. Residual contribution of the critical gap of E_c to the imaginary part of the dielectric constant for $\vec{E}\perp\vec{c}$ as a function of the temperature.

in the other polarization and we shall postpone the discussion about it to Sec. VI B.

B. Results for $\vec{E}$ parallel to $\vec{c}$ axis

At low energies we applied the same procedure as for the $\vec{E} \perp \vec{c}$ spectrum. However in this case, the results are less reliable, because we have to combine the experimental errors, the existence of tail states, and the fact that very soon we reach the region of the plateau in the absorption spectrum. So, we still get the same kind of energy dependence as for $\vec{E} \perp \vec{c}$, but the linear fit is only obtained over a range of 1500–2000 cm^{-1} of the absorption coefficient. From such a fit, we can infer the existence of an indirect gap between the M (or L) and Γ points. The energy of the phonon assisting the transition is found to be 260 ± 20 cm^{-1}, quite different from the one found for $\vec{E} \perp \vec{c}$. Following the preceding discussion it should be either the higher-energy TA phonon or the M_2^- LA phonon. In principle the large difference found between the energies of the two phonons (185 versus 260 cm^{-1}) should favor the proposal of a LA phonon assisting the transition for $\vec{E} \parallel \vec{c}$, but this should be confirmed by neutron scattering measurements which are not available at the present time.

The deduced gap $E_{g\parallel}$ has a value which is about 60 meV lower in energy than that found for $E_{g\perp}$. In this picture the plateau would correspond to a maximum in the energy dispersion curve of conduction levels.

If we assume that the band structure of PtS_2 is similar to that found by Mattheiss for $1T$-TaS_2 or $1T$-HfS_2, we should have at M or L the two valence levels lightly split, the higher-energy one being of the 1^+ symmetry (with a wave function of the d_{z^2} type) and the lower-energy level being of the 2^+ symmetry (with a wave function of the d_{xy} or $d_{x^2-y^2}$ type) (see Fig. 1). We should also have the lower conduction level at Γ with a 3^+ symmetry (wave functions of the d_{xz} and d_{yz} type). With such a scheme, $E_{g\perp}$ would measure the gap between the M_2^+ (or L_2^+) and Γ_3^+ levels and $E_{g\parallel}$ the gap between M_1^+ (or L_1^+) and Γ_3^+ level. The splitting between the 1^+ and 2^+ valence levels would be of 60 meV. The difference between the energy of the plateau and that of the $E_{g\parallel}$ gap can be interpreted as a measure of the dispersion of the conduction level parallel to the $\vec{c}$ axis that is the Γ-A direction in the Brillouin zone. This dispersion is found to be of the order of 0.3 eV.

All the preceding discussion is based on the assumption that the low-energy part of $\alpha_\parallel$ is given by interband electronic transitions. An alternative explanation for this part of the spectrum could be the existence of an absorption band due to the high density of defects in the semiconductor. We have rejected this explanation for the following reasons: (i) the strength of the absorption is quite high (5000 cm^{-1}) for such processes; (ii) the defects, mainly platinum vacancies, are probably deep impurities and the resulting absorption should not vary with temperature in the same way that interband transitions; (iii) it is difficult to understand why this absorption would be active for $\vec{E} \parallel \vec{c}$ and not for $\vec{E} \perp \vec{c}$. So we think that the low-energy spectrum of $\alpha_\parallel$ originates from interband electronic transitions.

The structure E_c appearing around 1.35 eV is also seen for the $\vec{E} \perp \vec{c}$ polarization. However the strength of the transition measured in terms of $\Delta\epsilon_2$ is quite different in both polarizations. We found $\Delta\epsilon_{2\parallel} \simeq 5$ and $\Delta\epsilon_{2\perp} = \epsilon'_{2\perp} \simeq 0.6$. This difference is typical of the transfer of some oscillator strength between polarized allowed and forbidden transitions, due to the spin-orbit interaction which mixes the selection rules. This transition is then probably only allowed for $\vec{E} \parallel \vec{c}$ axis when spin-orbit coupling is neglected. As this has already been pointed out, this transition should involve p-like levels in the conduction bands, and looking at the Mattheiss's scheme, one could assign it to a direct transition between the M (or L) valence levels to a M_2^- (or L_2^-) level which has a p_z-like function around the platinum. More specifically, it should characterize the $M_1^+ \rightarrow M_2^-$ or $L_1^+ \rightarrow L_2^-$ transition. The nature of this transition is not evident. From what we observe there is apparently no exciton formation or at least no excitonic lines around the singularity. But a free exciton would merge in a continuum of electronic transitions and/or could have a lifetime strongly shortened by the high density of defects in the crystal. So the absence of absorption lines does not necessarily mean that the observed edge is independent of excitonic effects. From what we know about the shape of ϵ_2 curves, this kind of edge can be explained as a M_1 singularity in a three-dimensional (3D) model or as a M_0 singularity in a two-dimensional (2D) model. The only difference is that ϵ_2 for a M_0 (2D) is a step function and that ϵ_2 for a M_1 (3D) varies below the critical energy E_c as $(E_c - E)^{1/2}$. The problem is that any relaxation effect would soften the step function. Moreover, the Mattheiss scheme for $1T$-TaS_2 or $1T$-HfS_2 predicts the existence of a M_0 point at L and a M_1 point at M. For these compounds the M_0 transition is found at an energy lower than the M_1 one, and this points to the existence of a two-dimensional M_0 critical point which has never been clearly observed experimentally up to now. However, only a band-structure calculation for PtS_2 could unambiguously answer the question.

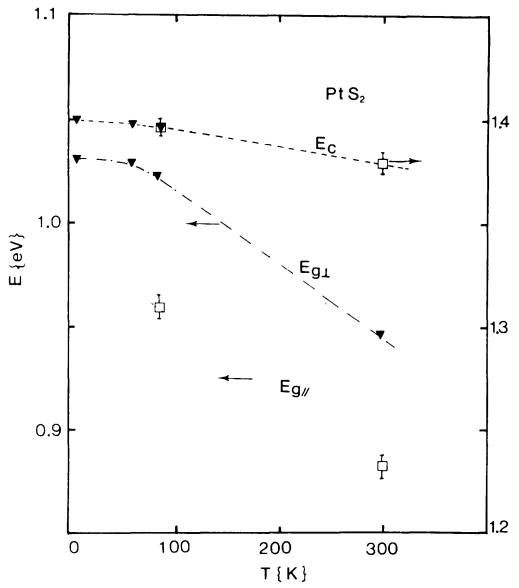

FIG. 8. Experimental variation of the observed electronic transitions as a function of the temperature. The left scale corresponds to the variation of $E_{g\perp}$ and $E_{g\parallel}$ with temperature. The right scale corresponds to the variation of E_c with temperature. Empty squares are measurements performed for $\vec{E} \parallel \vec{c}$ and black triangles measurements performed in the $\vec{E} \perp \vec{c}$ configuration.

C. Temperature dependence of the gaps

Results as a function of the temperature are gathered on Fig. 8. On the energy scale on the left are reproduced the variations of the indirect gaps $E_{g\perp}$ and $E_{g\parallel}$ with temperature. Between 85 and 300 K a mean temperature coefficient can be defined. Within experimental errors, this coefficient is found to be the same for both gaps: $\partial E_g/\partial T = (-3.7 \pm 0.2) \times 10^{-4}$ eV/K. With the right-hand energy scale, the variation of E_c is plotted as a function of the temperature. Within the same temperature range E_c appears to vary with a coefficient $\partial E_c/\partial T = (-7 \pm 0.5) \times 10^{-5}$ eV/K, much lower than $\partial E_g/\partial T$. This difference can be explained by the different symmetry of the levels involved in these two kinds of gaps. The negative sign of the coefficients is typical of what is found for all other lamellar semiconductors. These coefficients are composed of two parts: one is the extrinsic part due to the expansion of the lattice with temperature and the other part is the intrinsic contribution due to the electron-phonon interaction. The first part is usually known from the variation of the gap with pressure and from the thermal expansion coefficient. The intrinsic part is then deduced. Unfortunately we have no information about the pressure coefficients and the thermal expansion. All other lamellar semiconductors exhibit a negative pressure coefficient[12] which gives a positive contribution for the extrinsic part. So, the electron-phonon contribution to the temperature dependence of the gap is negative. We expect here a similar result. From what we know about the processes giving rise to this contribution, the negative sign can be explained by the predominance of the electronic intraband transitions with respect to the other processes. Allen and Heine[13] have shown that in the limit where the dispersion curves for the energy versus $\vec{k}$ vector is weak, which is the case for molecular crystals or roughly the case for lamellar compounds, the Debye-Waller effect and the interband processes compensate each other. The only significant contribution to the intrinsic part of the temperature coefficient is then given by the intraband processes, which always results in a negative sign for the coefficient. So, we expect this process to be dominant in this compound.

VII. CONCLUSION

We have reported experimental results on the optical properties of PtS_2 around the fundamental absorption edge for both $\vec{E}$ perpendicular and parallel to the $\vec{c}$ axis. Experimental results have been interpreted with a model involving a maximum of the valence bands at the M (or L) point and a minimum of the conduction levels at the Γ point. The indirect gaps occur for both polarizations between d states of the platinum. This situation explains why the high concentration of platinum vacancies does not provide an equivalent concentration of carriers in the system. The situation is probably close to that of a compensated material. Indirect transitions are assisted by odd parity phonons at the zone boundary of the Brillouin zone (M or L). A direct gap is found at higher energy, the transition being mainly allowed for $\vec{E} \parallel \vec{c}$.

A more detailed understanding of the character and the nature of these transitions should be provided by a band-structure calculation for this compound.

ACKNOWLEDGMENTS

We are indebted to Professor A. Wold and Dr. S. Soled for their contribution to the crystal growth of the compounds used in our experiments.

[1]A. Finley, D. Schleich, J. Ackermann, S. Soled, and A. Wold, Mater. Res. Bull. 9, 1655 (1974).
[2]M. Zanini, American Physical Society Meeting, March 1976 (unpublished).
[3]R. W. G. Wyckoff, *Crystal Structure*, 2nd ed. (Interscience, New York, 1965), Vol. 1, p. 269.
[4]N. Piccioli, R. Le Toullec, M. Mejatty, and M. Balkanski, Appl. Opt. 16, 1236 (1977).
[5]L. F. Mattheiss, Phys. Rev. B 8, 3719 (1973).
[6]J. B. Goodenough, Phys. Rev. 171, 466 (1968).
[7]R. Huisman, R. Dejonge, C. Haas, and J. Jellinek, J. Solid State Chem. 3, 56 (1971).
[8]See for instance S. Sugano, Y. Tanabe, and H. Kamimura, *Multiplets of Transition Metal Ions in Crystals* (Academic, New York, 1970).
[9]R. Le Toullec, N. Piccioli, M. Mejatty, and M. Balkanski, Nuovo Cimento B 63, 45 (1969), and references therein.
[10]K. Nakao, H. Kamimura, and Y. Nishina, Nuovo Cimento B 63, 45 (1969), and references therein.
[11]M. Lax and J. J. Hopfield, Phys. Rev. 124, 115 (1961).
[12]J. M. Besson, Nuovo Cimento (to be published).
[13]P. B. Allen and V. Heine, J. Phys. C 9, 2305 (1976).